Published in Applied Optics 34, issue 14, 2540-2547, 1995
which should be used for any reference to this work

Interferometric fabrication of modulated submicrometer gratings in photoresist

Peter Ehbets, Hans Peter Herzig, Philippe Nussbaum, Peter Blattner, and René Dändliker

Interferometric recording is applied to the fabrication of modulated submicrometer gratings in photoresist. High diffraction efficiency requires optimized recording conditions, which are obtained by the use of an on-axis continuous surface-relief grating for the generation of the object beam. The optimized phase function is copied into the resist layer by means of a self-aligned two-step recording process with an intermediate copy in a volume photopolymer hologram. As a result, we demonstrate high carrier frequency surface-relief off-axis fan-out gratings for illumination in transmission with visible light.

Key words: Holography, photoresist, submicrometer gratings, diffractive optical elements, optical interconnects.

1. Introduction

Modern microfabrication techniques permit the realization of highly efficient diffractive optical elements (DOE's) that have multilevel or continuous microreliefs.[1] However, difficulties still arise for the fabrication of off-axis elements in rigid materials such as glass or quartz with submicrometer carrier grating periods. These elements are of interest for building compact optical systems with a folded optical path.[2] Furthermore, they are attractive because high efficiency can already be achieved with a two-level phase profile. Therefore recent research has focused on the design and fabrication of modulated high carrier frequency gratings.[3–5]

Modulated submicrometer gratings have been fabricated by use of electron-beam (e-beam) lithography for the patterning of the resist. This technique offers high flexibility for the generation of arbitrary structures. The accuracy of e-beam writing is mainly limited by stitching errors of the order of 100 μm between scan fields when the elements exceed the size of a single scan field, i.e., when they are larger than 0.8–1.0 mm.[6] Within one scan field the positioning errors are typically of the order of 10–50 nm. These positioning errors introduce detour phase factors for off-axis elements that affect the encoded object phase function and limit the performance in the case of submicrometer carrier grating periods.[4]

Here we present an alternative fabrication method for binary off-axis DOE's based on optimized interferometric recording in photoresist. This approach has the advantage of a parallel writing process that can be used directly for the fabrication of larger quantities. In addition, wave fronts can be generated with high accuracy over large fields, which results in a better positioning accuracy of the modulated grating lines. However, interferometric recording is less flexible compared with e-beam writing.

Most of the research in photoresist recording has involved the fabrication of regular, high-resolution gratings. Conditions for high first-order diffraction efficiency have been derived and experimentally demonstrated.[7–10] However, only a few studies have investigated the recording of more general object beams in photoresist. The recording of photoresist holograms was studied by Bartolini.[11] He observed a strong trade-off between efficiency and reconstruction fidelity and could achieve only low efficiencies of the order of 5%. The reconstruction fidelity is mainly affected by the intermodulation noise, which is due to the recorded object-beam intensity variations in the hologram. Better performance can only be achieved if these intermodulations are reduced or even eliminated. For the recording this requires the use of optimized object beams, which can in general be produced by computer-generated holograms. The

The authors are with the Institute of Microtechnology, University of Neuchâtel, Rue Breguet 2, Neuchâtel CH-2000, Neuchâtel, Switzerland.

copying of an optimized wave front with an off-axis reference beam into a hologram led to the concept of hybrid holograms.[12] Bartelt and Case[12] achieved diffraction efficiencies of the order of 50% and good fidelity by recording an object beam with random phase in a volume hologram. High diffraction efficiencies over 90% were then obtained for the copying of fan-out elements in dichromated gelatin.[13,14] In this case the intermodulations were minimized by the application of numerical optimization techniques. We have applied the same concept for the recording of efficient surface-relief holograms in photoresist.

In Section 2 we discuss the recording conditions for efficient photoresist holograms. In Section 3 the generation of optimized object beams is considered and the recording setup for the copying is discussed. Accurate positioning of the photoresist plate in the optimum recording plane is crucial. To achieve precise alignment we applied a two-step approach for the copying. In Section 4 experimental results are presented for the fabrication of an off-axis 9 × 9 fan-out element. Fan-out elements are key components for optical interconnects. In this research we use them as test elements, because the generated spot array in the far field of the fan-out element can be easily characterized. The accuracy of the fabrication process can be deduced from the uniformity error of the generated array.

2. Optimized Holographic Recording in Photoresist

The basic configuration for interferometric recording is shown in Fig. 1. The interference pattern of a plane reference wave and an object beam is recorded in a thin photoresist layer. Symmetric incidence of the two beams is required in order to produce interference fringes perpendicular to the hologram plane. Incidence angle θ defines the period of carrier grating s with $s = \lambda/(2 \sin \theta)$, where λ is the free-space wavelength of the recording light. After development a modulated surface-relief grating is obtained. At readout the grating is illuminated at Bragg angle θ_B, which is defined by $\sin \theta_B = \lambda/(2s)$. The object-beam wave front is regenerated in the minus-first diffraction order of the carrier grating and produces the desired intensity pattern in the far field. In the case of high carrier frequency gratings, the angular spread of the object beam, α, is much smaller compared with Bragg angle θ_B.

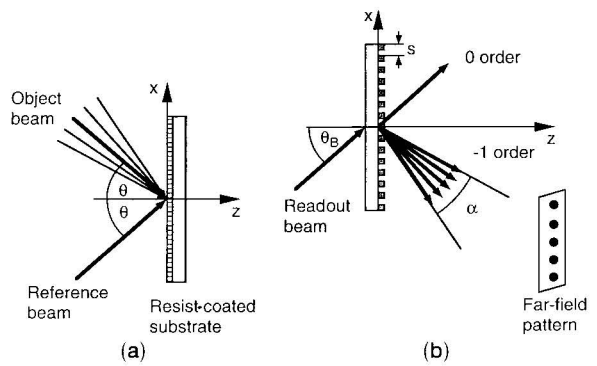

Fig. 1. Geometries of (a) recording and (b) readout for interferometric recording in photoresist.

We restrict the following analysis to one-dimensional object beams, but the same principle can be applied to the two-dimensional case. The plane of incidence is the (x, z) plane as shown in Fig. 1, and TE polarization is assumed. The reference plane wave can then be written as

$$E_r(x, z) = A_r \exp\{ik[\sin(\theta)x + \cos(\theta)z]\}, \quad (1)$$

where $k = 2\pi/\lambda$. The electric field of the object beam can be expressed by a spatially varying amplitude and phase function, i.e.,

$$E_o(x, z) = \exp[-ik \sin(\theta)x]A_o(x, z)\exp[i\Phi_o(x, z)], \quad (2)$$

where the linear phase factor determines the off-axis incidence. In the general case the propagation of Eq. (2) can be calculated by the use of the angular spectrum approach.[15] We are particularly interested in the recording of fan-out gratings. In this case the object amplitude and phase functions, $A_o(x, z)$ and $\Phi_o(x, z)$, are periodic with respect to the x axis and can be written as a discrete superposition of propagating diffraction orders, i.e.,

$$E_o(x, z) = \exp[-ik \sin(\theta)x] \sum_{m=-M}^{N} A_m \exp(i\varphi_m) \times \exp[i(mKx + \gamma_m z)], \quad (3)$$

where $(M + N + 1)$ is the total number of diffraction orders retained in the analysis, $K = 2\pi/\Lambda$, Λ is the period of the fan-out element, and γ_m is the propagation constant of the mth diffraction order along the z axis, defined by

$$\gamma_m = \{k^2 - [k \sin(\theta) + mK]^2\}^{1/2}. \quad (4)$$

The diffraction orders are characterized by their amplitudes, A_m, and phases, φ_m. The central N_s diffraction orders form the fan-out signal and create the spot array in the Fourier plane. All the higher diffraction orders correspond to undesired noise. The quality of a fan-out element is characterized by two parameters: the signal diffraction efficiency, η, and the uniformity error, e, of the generated array. The signal diffraction efficiency is the fraction of the total power in the N_s signal diffraction orders. Uniformity error e can be defined by the contrast function,

$$e = \frac{I_{\max} - I_{\min}}{I_{\max} + I_{\min}}, \quad (5)$$

where $I_{\max}$ and $I_{\min}$ are the maximum and minimum spot intensities of the N_s signal beams.

Using Eqs. (1) and (2) we can write the interference of the reference wave with the modulated object beam

in a form similar to the two-wave case, i.e.,

$$I(x, z) = |E_r(x, z) + E_o(x, z)|^2$$
$$= A_r^2 + A_o(x, z)^2 + 2A_rA_o(x, z)$$
$$\times \cos[Qx - \Phi_o(x, z)], \quad (6)$$

where $Q = 2\pi/s = 2k \sin \theta$. Optimized recording conditions are obtained if the intensity variations of object-beam amplitude $A_o(x, z)$ are minimized in the hologram plane at $z = 0$. This is identical to the design of an on-axis phase-only DOE. Assuming $A_o(x, z)$ and $\Phi_o(x, z)$ to be slowly varying with respect to the wavelength λ, we can apply the paraxial scalar diffraction theory. Many different optimization schemes have been proposed in the literature for this task, based on either iterative phase-retrieval algorithms[16–18] or parametric optimization techniques.[19] In the case of regular fan-out elements, continuous phase functions as shown in Fig. 2 for a 9 × 1 fan-out element can be determined.[20] This phase-only solution produces in the far field a uniform spot array with a high signal diffraction efficiency of 99.3%. The corresponding interference pattern of Eq. (6) is shown in Fig. 3. For the representation, a low carrier frequency $Q = 4\pi N_s/\Lambda$ has been chosen. The whole object information is encoded in phase function $\Phi_o(x, z = 0)$, which modulates frequency Q of the carrier grating.

The recorded sinusoidal intensity distribution, shown in Fig. 3, is transformed by the photoresist development into a surface-relief grating. The physics of the photoresist development process is described in Ref. 11. Depending on the type of developer and the dilution, either a binary or a rather linear characteristic between the exposure energy and the photoresist relief depth can be achieved. In the case of binary development the sinusoidal interference pattern is hard clipped, and a rectangular-shaped surface relief results. For linear development the sinusoidal form is more or less maintained. It has been shown that high diffraction efficiencies with a rectangular or sinusoidal grating require carrier grating periods of the order of the optical

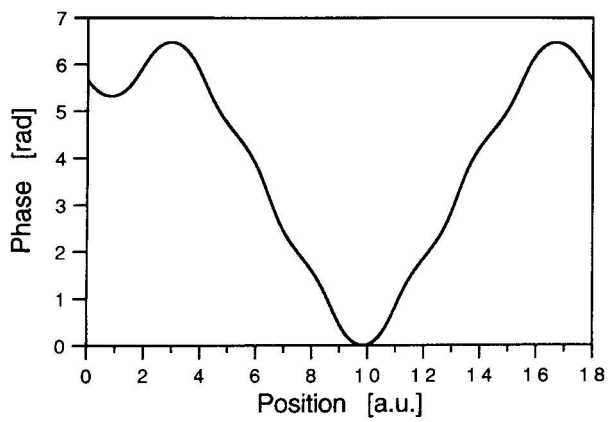

Fig. 2. One period of the optimized phase function for an on-axis 9 × 1 fan-out element.

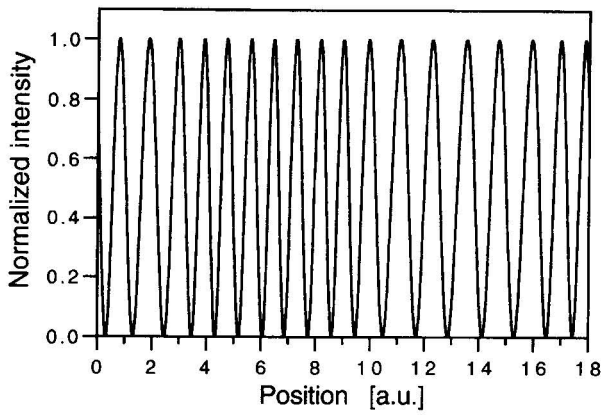

Fig. 3. One period of the optimized interference pattern in the recording plane for the 9 × 1 fan-out element.

wavelength.[7,10] In this case only the zeroth and the minus-first diffraction order are propagating for incidence at the Bragg angle. As a consequence the diffraction at the high frequency carrier surface-relief grating has to be analyzed by the use of rigorous diffraction theories. This is a demanding task because the period of the modulated grating is defined by the period of the paraxial object function, which typically has a size of $\Lambda > 100$ μm. As a consequence, a large number of diffraction orders has to be retained in the model. A rigorous analysis of this type of binary high frequency carrier DOE's was recently published by Noponen and Turunen.[3] They analyzed the validity of the hybrid encoding scheme and found that the fan-out phase function would be correctly encoded in the binary carrier grating if the period of the highest frequency component in the fan-out function was at least 10 times larger than the period of carrier grating s, i.e.,

$$\frac{\Lambda}{N_s s} > 10. \quad (7)$$

In the reported experiments we use a factor 10 above this limitation, and therefore encoding errors can be neglected. The first-order diffraction efficiency is then optimized by the consideration of the regular carrier grating. We used a model based on rigorous coupled-wave theory[7] and determined the optimum relief depth, h, of the grating for TE polarization. The efficiency curves are shown in Fig. 4 for the two cases of a rectangular and a sinusoidal relief profile illuminated in transmission from resist to air at the Bragg angle. The results were calculated for a wavelength of $\lambda = 633$ nm, a typical photoresist index of $n = 1.63$, and a grating period of $s = 577.4$ nm. High diffraction efficiencies over 90% can be achieved for both relief types and require a modulation depth in the range of 0.8 μm $< h <$ 1.0 μm.

Optimized phases of the recording fan-out beam achieve minimum intermodulations in a single plane ($z = 0$). As the object beam propagates out of this optimum plane, intermodulations will appear and deteriorate the recording conditions. To specify the

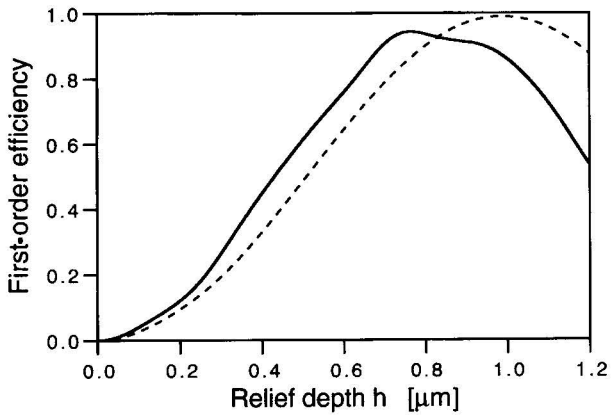

Fig. 4. Calculated first-order diffraction efficiency η_{-1} as a function of relief depth h for a rectangular relief profile (solid curve) and for a sinusoidal relief profile (dashed curve).

alignment tolerances for a successful recording, we determined the depth of the optimum plane. The propagation of the object beam is described by Eqs. (3) and (4). We assumed off-axis propagation at a recording angle of $\theta = 25°$ and calculated the evolution of the intermodulations $A_o(x, z)$ for the optimized 9×1 fan-out element, shown in Fig. 2. The calculated contrast of intermodulations V resulting from a displacement $z = d$ out of the optimum plane is shown in Fig. 5 for different fan-out periodicities Λ equal to 100, 200, and 400 μm. Intermodulation contrast V was defined by $V = (I_{max} - I_{min})/(I\ max + I_{min})$, where I_{max} and I_{min} are the maximum and minimum intensities of the object beam in the plane $z = d$. Gratings recorded under the conditions for high diffraction efficiency cannot linearly reproduce object intermodulations $A_o(x, z = d)$. Small intensity variations caused by intermodulations are clipped to a constant value because of nonlinear development and because of the strongly nonlinear behavior of the diffraction efficiency curve near its maximum. However, object phase function $\Phi_o(x, z = d)$ is accurately recorded by the relative phase of the carrier grating. The clipping of the amplitude function to $A_o(x, z = d) = \text{const.}$ discards some object information.

The result of the clipping can best be analyzed by the calculation of the uniformity error of the spot array generated from phase-only function $\Phi_o(x, z = d)$. The results are shown in Fig. 6. For most applications a uniformity error of $e < \pm 10\%$ can be tolerated. Therefore, using Figs. 5 and 6, one can estimate the depth of the optimum plane and tolerable clipping level. Significant intermodulations occur of the diffraction orders at the border of the fan out loose the optimum phase relation with the central beam. The interference between one marginal diffraction order of the fan out and the central fan-out beam results in a periodic function. The period of this interference pattern in the direction of the z axis gives a good estimation for the depth of the optimum recording plane. For small fan-out angles α, the relation

$$t = c\,\frac{\cos(\theta)\Lambda^2}{\pi\lambda N^2} \tag{7}$$

is obtained for the depth as a function of the fan-out parameters, where c is a constant defined by the tolerable uniformity error and $N \approx (N_s - 1)/2$. The depth of the optimum plane is mainly determined by the quadratic dependence on fan-out period Λ and on the number of signal diffraction orders N_s. Oblique incidence at angle θ results only in the cosine factor and has little influence.

3. Two-Step Recording Setup

The problems at recording are the generation and the accurate alignment of the optimized object beam with respect to the hologram plane. Different possibilities exist for the generation of the optimized object beam in the hybrid recording arrangement introduced by Bartelt and Case. The most common approach is to encode the optimized wave front in a low-resolution computer-generated hologram[13,20] and then copy it in the hologram plane by means of a $4f$ imaging system. For the generation of large spot

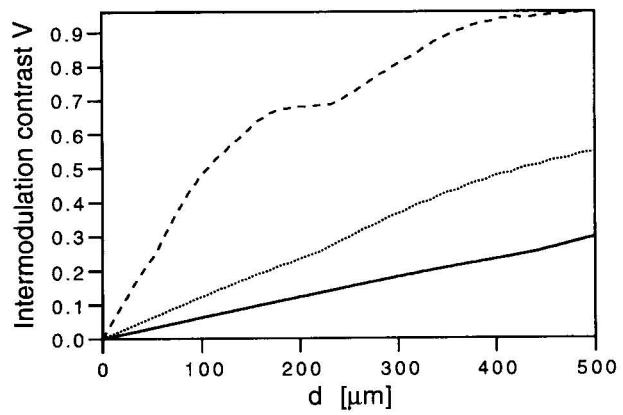

Fig. 5. Contrast V of the intermodulations as a function of displacement d out of the optimum plane calculated for different fan-out periods of $\Lambda = 100$ μm (dashed curve), $\Lambda = 200$ μm (dotted curve), and $\Lambda = 400$ μm (solid curve).

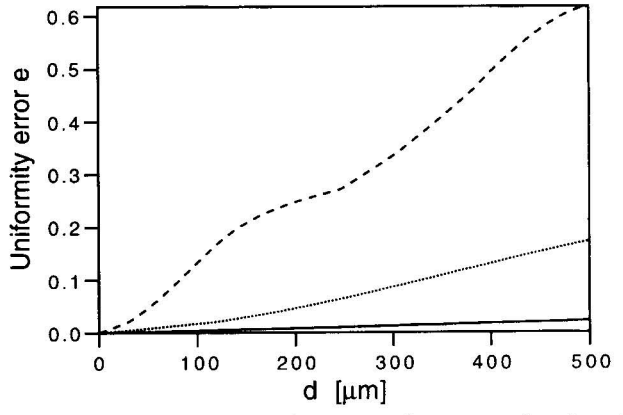

Fig. 6. Uniformity error e of the generated array as a function of displacement d out of the optimum plane calculated for different fan-out periods of $\Lambda = 100$ μm (dashed curve), $\Lambda = 200$ μm (dotted curve), and $\Lambda = 400$ μm (solid curve).

arrays, the self-imaging properties of periodic fields become interesting. By considering the free-space propagation after a pinhole array, one can find planes of low intermodulations.[21] In this research we chose a third approach by copying the optimized phase function of an existing on-axis phase-only DOE into the hologram plane. Problems appear with the hybrid recording approach if, for the desired far-field pattern, phase functions with low diffraction efficiencies are found. In this case higher diffraction orders besides the N_s signal diffraction orders become important and are necessary to describe the phase-only solution. As a consequence, spatial filtering of the imaging system has to be taken into account to achieve low intermodulation.[13] For regular, discrete patterns such as fan-out elements, high diffraction efficiencies can be achieved with continuous or multilevel DOE's. In the reported experiment we used a continuous surface-relief grating as the master element for the interferometric copying. The fabrication of continuous surface-relief gratings is a critical process, but good results have been obtained by laser-beam writing.[22]

For the required relief depth for transmission gratings to be achieved, interference fringes perpendicular to the resist surface are required. Therefore, the optimized plane of low-intensity variations is tilted with respect to the propagation direction of the object beam, and the alignment of the imaging system becomes a difficult task. The alignment tolerances are shown in Fig. 6 and can be estimated from relation (7). We have avoided these problems by using a two-step recording approach for the copying. The two-step recording process is schematically represented in Figs. 7 and 8. The optimized phase function of the on-axis fan-out element is first copied in a volume hologram. This intermediate copy does not have to be recorded for high diffraction efficiency. Therefore a linear recording process can be used, which can restore the intermodulations.[12] This hologram is recorded with a high reference-to-object-beam ratio. As we can see in Fig. 7, we imaged fan-out phase function $\Phi_o(x, z = 0)$ into the hologram plane by using a single lens. This transformation adds a quadratic phase term to the fan-out phase but introduces no intensity variations.

Because of the linear recording conditions of the volume hologram, small intermodulations can be tolerated, and the alignment requirements in the

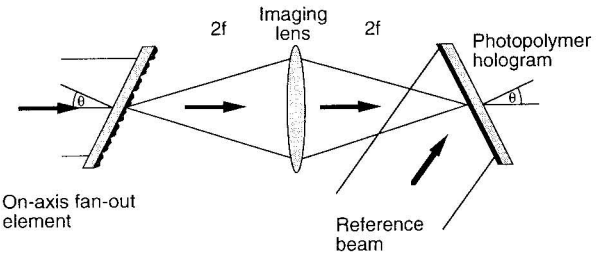

Fig. 7. Recording geometry of the intermediate copy in the photopolymer hologram.

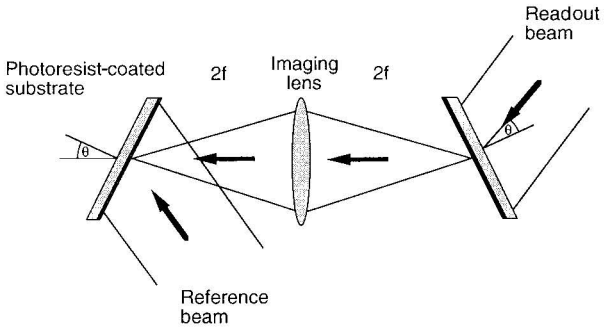

Fig. 8. Recording geometry of the resist hologram.

image plane become less severe. We used a photopolymer as the holographic recording medium for the intermediate copy. The photopolymer material has the advantage that it is self-developing during the exposure. The holographic plate can therefore be kept in place during the whole process and is automatically aligned. At readout the photopolymer hologram is illuminated by the conjugate reference beam, as shown in Fig. 8. This illumination generates the conjugate object beam, which passes inversely through the same imaging system and compensates on its way all the acquired aberrations. The complex conjugate of the fan-out phase function, i.e., $-\Phi_o(x, z = 0)$, is then reconstructed in the plane where the original fan-out element was placed. The Fourier transform properties show that complex conjugation of a phase function introduces an inversion symmetry in the far field, but it does not change the intensity distribution. As a result, the conjugate phase function is again a uniform fan-out element and the photoresist hologram can be recorded in this predefined plane with a symmetric off-axis reference beam.

4. Experimental Results

Experimental results were obtained by the use of this two-step recording approach for copying a continuous surface-relief 9 × 9 fan-out element into a modulated binary resist grating. We obtained the two-dimensional phase function by crossing two symmetric one-dimensional solutions, which are shown in Fig. 2. The design and the fabrication by laser-beam writing of this element have been described in previous publications.[22,23] The fan-out gratings were realized with a period of $\Lambda = 400$ μm and for a wavelength of $\lambda = 488$ nm. For normal incidence, phase function $\Phi_o(x, z = 0)$ and relief height $d(x)$ are related by

$$\Phi_o(x, z = 0) = \frac{2\pi}{\lambda}(n - 1)d(x), \tag{8}$$

where n is the refractive index of the medium. Propagation through the same phase grating at oblique incidence results in phase modulation errors. The main error is a linear increase of the optical path length difference, which can be compensated by the rescaling of relief profile $d(x)$ calculated for normal incidence. The corrected relief height $d_c(x)$ for ob-

lique incidence is obtained by

$$d_c(x) = d(x)\frac{n-1}{n\cos(\theta_n) - \cos(\theta)}, \qquad (9)$$

where θ and θ_n are the incidence angles in air and in the medium. In general, higher-order phase errors will appear. Because of the large ratio between the fan-out period and the modulation depth, these local phase deformations are smaller than $\pi/100$ and thus far below the fabrication accuracy. We fabricated a continuous surface-relief 9 × 9 fan-out element in photoresist with a refractive index of $n = 1.64$ for the required recording angle of $\theta = 25°$. This requires a relief depth correction, Eq. (9), of 0.94. The far-field characterization of the fabricated element yields a uniformity error of $e = \pm 10\%$ over the whole 9 × 9 array.

For the imaging system shown in Fig. 7, a lens with focal length of $f = 100$ mm and an aperture diameter of 50 mm were chosen. With this configuration, spatial filtering effects can be neglected. The intermediate volume hologram copy was made in the photopolymer material HRS352 from Du Pont de Nemours[24] by the use of an argon laser at the wavelength $\lambda = 488$ nm. The photopolymer layer was spin coated to a thickness of 17 μm on a BK-7 glass substrate with antireflection coating on the opposite surface. Symmetric incidence between the reference beam and the object beam was chosen for the recording. Because the image plane of the fan-out element is again a plane of low intermodulations, a high reference-to-object-beam ratio is not necessary for a linear recording process.[25] We used a beam ratio equal to unity. Typical exposure parameters have been an energy of $E = 150$ mJ/cm^2, followed by a diffusion time of ~8 min, and a uniform postexposure to fix the hologram. Efficiencies of the order of 40% were obtained without heating the photopolymer hologram after exposure. Under these conditions an excellent linear recording was achieved. The intermediate photopolymer hologram reconstructed the 9 × 9 spot array in the far field with the same uniformity error as the original fan-out element.

The final copy was made in Shipley Microposit 1400-37 photoresist. A layer of 2.8 μm thickness was spin coated on a glass substrate and baked at 95 °C for 30 min. For the exposure an absorber was index matched on the backside of the substrate to avoid backreflections, and symmetric incidence at ±25° was chosen. Because the photoresist material has low sensitivity at the wavelength of $\lambda = 488$ nm, high exposure energies of the order of 1.5 J/cm^2 are required. The consequence of using expanded beams are exposure times of several minutes. Under these circumstances, fringe stabilization becomes important. We obtained the best performance by stabilizing the large interference fringes produced from a reference grating with equal period, which was fixed on the same substrate holder. During the exposure the piezocorrection signal of the fringe stabilization system varied by the order of $\lambda/20$. Because the average position of the fringes is recorded, the position accuracy of the recorded pattern is still better. After exposure the resist holograms were developed during 30 s in the AZ-303 developer from Hoechst diluted 1:4. According to Bartolini,[11] this process results in rather linear development characteristics. The form of the resulting surface relief for a modulated fan-out grating can be seen on the scanning electron microscopy picture of Fig. 9. Grating period $s = \lambda/(2\sin\theta) = 577.4$ nm results from the incidence angle of $\theta = 25°$. We achieved maximum relief depths of the order of 600 nm by using this process. The position modulation of the grating grooves is only of some nanometers and cannot be distinguished in Fig. 9.

The modulated fan-out gratings were designed for readout in transmission with the He–Ne laser wavelength $\lambda = 633$ nm. The achieved relief depths of 600 nm are not optimum, as one can seen from the efficiency curves in Fig. 4. The wavelength change between recording and readout shifts the Bragg angle to $\theta_B = \lambda/(2s) = 33.2°$. An overall first-order efficiency of $\eta_{-1} = 69\%$ was measured for the grating shown in Fig. 9. This value includes the Fresnel reflection loss of $R = 6\%$ at the first substrate interface and absorption of the order of 2% in the photoresist. The generated 9 × 9 spot array in the far field of the minus-first diffraction order is shown in Fig. 10. The CCD picture is saturated so that the small sidelobes of the Airy function around each spot are visible. One can see that no significant higher diffraction orders appear outside of the signal array. The 9 × 9 spot array contains 65% of the total incident power. The 4% efficiency loss compared with the first order efficiency is mainly due to light that is scattered at the rough photoresist surface. The surface roughness results from coherent noise that is generated from backreflections. Improvements are possible by the reduction of the coherence length of the recording laser and by the use of an incoherent preexposure. The uniformity of the array was measured for illumination with a collimated

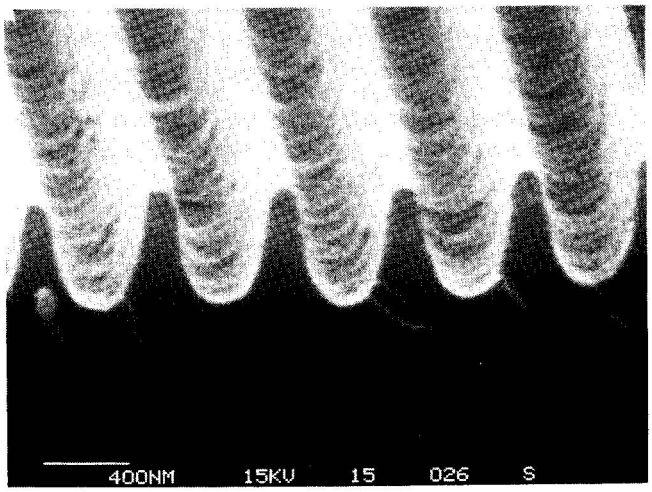

Fig. 9. Scanning electron microscopy picture of the fabricated surface relief in photoresist.

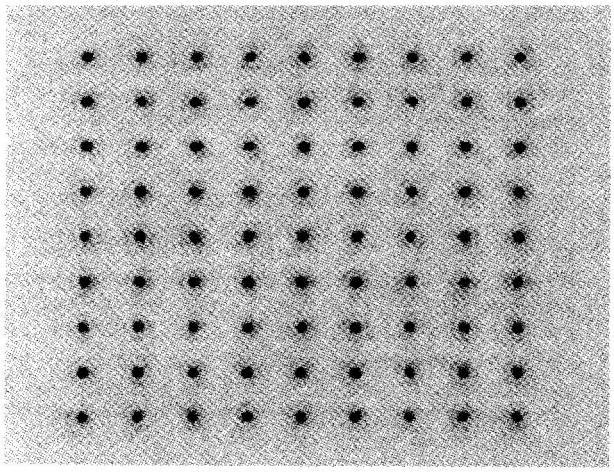

Fig. 10. 9 × 9 array of generated spots in the minus-first diffraction order of the carrier grating.

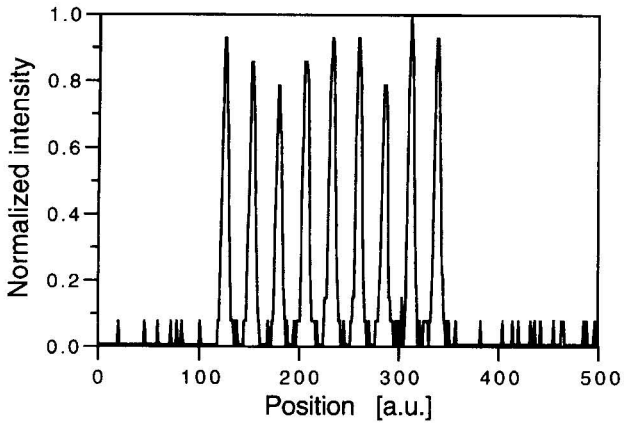

Fig. 11. Intensity line scan through the row of the 9 × 9 array with the highest uniformity error.

beam that was 4 mm in diameter. Each row of the array was scanned individually by a detector. The intensity distribution of the row with the worst uniformity is shown in Fig. 11. We measured a uniformity error of $e = \pm 13\%$. Compared with the uniformity error of $e = \pm 10\%$ of the original fan-out element, we achieved an accurate copy of the fan-out phase function. Higher diffraction efficiencies require slightly deeper relief depths. One can obtain this by improving the photoresist processing or by etching the binary resist relief in the substrate material.[1]

5. Conclusions

We investigated interferometric recording for the fabrication of modulated binary gratings with submicrometer periods in photoresist. Optimized recording conditions require minimum intermodulations in the hologram plane. This was achieved when the optimized phase function of an on-axis phase-only DOE was copied into the hologram plane. Alignment problems were solved by the use of an intermediate copy in a volume photopolymer hologram. After development a modulated binary surface-relief grating results, which can be transferred in a stable substrate material by the use of etching or material deposition techniques and which is also suitable for mass replication. The method has the potential to achieve ultrahigh carrier frequencies with high position accuracy. The far-field copying arrangement works well for object beams with high signal diffraction efficiencies. Off-axis 9 × 9 fan-out elements in transmission with a carrier frequency of 1700 lines/mm and first-order diffraction efficiencies in the range of 70% are demonstrated. Because of the high carrier frequency, these elements clearly show Bragg diffraction behavior and offer high first-order diffraction efficiency. Because they are thinner compared with standard volume holograms, they are much less sensitive to deviations of the readout angle. Therefore, these elements are interesting for optical interconnection systems, which require the generation of the fan-out signal not only for readout with a single reference beam but also for readout with a more complex input pattern.[26]

References

1. H. P. Herzig, M. T. Gale, H. W. Lehmann, and R. Morf, "Diffractive components: computer-generated elements," in *Perspectives for Parallel Optical Interconnects,* Ph. Lalanne and P. Chavel, eds. (Springer-Verlag, New York, 1993), pp. 71–107.
2. D. Prongué and H. P. Herzig, "Total internal reflection holography for optical interconnections," Opt. Eng. **33,** 636–642 (1994).
3. E. Noponen and J. Turunen, "Binary high-frequency-carrier diffractive optical elements: electromagnetic theory," J. Opt. Soc. Am. A **11,** 1097–1109 (1994).
4. J. Turunen, P. Blair, J. M. Miller, M. R. Tagizadeh, and E. Noponen, "Bragg holograms with binary surface-relief profile," Opt. Lett. **18,** 1022–1024 (1993).
5. E. Tervonen, J. Turunen, and J. Pekola, "Pulse-frequency-modulated high-frequency-carrier diffractive elements for pattern projection," Opt. Eng. **33,** 2579–2587 (1994).
6. M. J. Verheijen, "E-beam lithography for digital holograms," J. Modern Opt. **40,** 711–721 (1993).
7. M. G. Moharam and T. K. Gaylord, "Diffraction analysis of dielectric surface-relief gratings," J. Opt. Soc. Am. **72,** 1385–1392 (1982).
8. R. C. Enger and S. K. Case, "High-frequency holographic transmission gratings in photoresist," J. Opt. Soc. Am. **73,** 1113–1118 (1983).
9. M. G. Moharam, T. K. Gaylord, G. T. Sincerbox, and B. Yung, "Diffraction characteristics of photoresist surface-relief gratings," Appl. Opt. **23,** 3214–3220 (1984).
10. K. Yokomori, "Dielectric surface-relief gratings with high diffraction efficiency," Appl. Opt. **23,** 2303–2310 (1984).
11. R. A. Bartolini, "Characteristics of relief phase holograms recorded in photoresist," Appl. Opt. **13,** 129–139 (1974).
12. H. Bartelt and S. K. Case, "High-efficiency hybrid computer generated holograms," Appl. Opt. **21,** 2886–2890 (1982).
13. B. Robertson, J. Turunen, H. Ichikawa, J. M. Miller, M. R. Tagizadeh, and A. Vasara, "Hybrid kinoform fanout holograms in dichromated gelatin," Appl. Opt. **30,** 3711–3720 (1991).
14. H. P. Herzig and R. Dändliker, "Diffractive components: holographic optical elements," in *Perspectives for Parallel*

Optical Interconnects, Ph. Lalanne and P. Chavel, eds. (Springer-Verlag, New York, 1993), pp. 43–69.
15. J. W. Goodmann, *Introduction to Fourier Optics* (McGraw-Hill, New York, 1968), pp. 48–54.
16. R. W. Gerchberg and W. O. Saxton, "A practical algorithm for determination of phase from image and diffraction plane pictures," Optik (Stuttgart) **35,** 237–246 (1972).
17. J. R. Fienup, "Iterative method applied to image reconstruction and to computer-generated holograms," Opt. Eng. **19,** 297–305 (1980).
18. F. Wyrowski and O. Bryngdahl, "Iterative Fourier-transform algorithm applied to computer holography," J. Opt. Soc. Am. A **5,** 1058–1065 (1988).
19. J. Turunen, A. Vasara, and J. Westerholm, "Kinoform phase relief synthesis: a stochastic method," Opt. Eng. **28,** 1162–1167 (1989).
20. H. P. Herzig, D. Prongué, and R. Dändliker, "Optimized kinoform structures for highly efficient fan-out elements," Jpn. J. Appl. Phys. **27,** 1307–1309 (1990).
21. I. Seyd-Darwisch, J. Taboury, and P. Chavel, "Recording conditions of an array-illuminator hologram based on the Talbot effect," Appl. Opt. **32,** 7135–7144 (1993).
22. M. T. Gale, M. Rossi, H. Schütz, P. Ehbets, H. P. Herzig, and D. Prongué, "Continuous-relief diffractive optical elements for two-dimensional array generation," Appl. Opt. **32,** 2526–2533 (1993).
23. P. Ehbets, H. P. Herzig, D. Prongué, and M. T. Gale, "High-efficient continuous surface-relief gratings for two-dimensional array generation," Opt. Lett. **17,** 908–910 (1992).
24. W. J. Gambogi, W. A. Gerstadt, S. R. Mackara, and A. M. Weber, "Holographic transmission elements using improved photopolymer films," in *Computer and Optically Generated Holographic Optics,* I. Cindrich and S. H. Lee, eds., Proc. Soc. Photo-Opt. Instrum. Eng. **1555,** 256–267 (1991).
25. H. P. Herzig, P. Ehbets, D. Prongué, and R. Dändliker, "Fan-out elements recorded as volume holograms: optimized recording conditions," Appl. Opt. **31,** 5716–5723 (1992).
26. A. V. Krishnamoorthy, G. Yayla, and S. C. Esener, "A scalable optoelectronic neural system using free-space optical interconnects," IEEE Trans. Neural Net. **3,** 404–413 (1992).